



**HAL**  
open science

# Fast Computational Dynamic Model of Traction Drive for Electric Vehicles

Anatole Desreaveaux, Eric Labouré, Olivier Béthoux, Clement Mayet, Alessio Iovine, William Pasillas-Lépine, Francis Roy

► **To cite this version:**

Anatole Desreaveaux, Eric Labouré, Olivier Béthoux, Clement Mayet, Alessio Iovine, et al.. Fast Computational Dynamic Model of Traction Drive for Electric Vehicles. 2022 IEEE Vehicle Power and Propulsion Conference (VPPC 2022), Nov 2022, Merced, United States. 10.1109/VPPC55846.2022.10003383 . hal-03872463

**HAL Id: hal-03872463**

**<https://hal.science/hal-03872463>**

Submitted on 25 Nov 2022

**HAL** is a multi-disciplinary open access archive for the deposit and dissemination of scientific research documents, whether they are published or not. The documents may come from teaching and research institutions in France or abroad, or from public or private research centers.

L'archive ouverte pluridisciplinaire **HAL**, est destinée au dépôt et à la diffusion de documents scientifiques de niveau recherche, publiés ou non, émanant des établissements d'enseignement et de recherche français ou étrangers, des laboratoires publics ou privés.

# Fast Computational Dynamic Model of Traction Drive for Electric Vehicles

A. Desreuveaux<sup>1,2,3</sup>, E. Labouré<sup>1,2</sup>, O. Bethoux<sup>1,2</sup>, C. Mayet<sup>4</sup>, A. Iovine<sup>3</sup>, W. Pasillas-Lepine<sup>3</sup>, F. Roy<sup>5</sup>

1. Université Paris-Saclay, CentraleSupélec, CNRS, Laboratoire de Génie Electrique et Electronique de Paris, 91192, Gif-sur-Yvette, France.
2. Sorbonne Université, CNRS, Laboratoire de Génie Electrique et Electronique de Paris, 75252, Paris, France
3. Laboratoire des signaux et systèmes (L2S), Université Paris-Saclay, CNRS, CentraleSupélec, 91190, Gif-sur-Yvette, France.
4. SATIE, UMR CNRS 8029, Le Cnam, F 75003 Paris, France
5. Stellantis, Automotive Research and advanced engineering, 78943 VELIZY VILLACOUBLAY, France

**Abstract**— To reduce the time-to-market of electric vehicles, fast and accurate energetic simulations are needed. This paper aims to propose a fast computational dynamic model that allows a good compromise between accuracy and computation time while respecting the dynamics of the system. Its accuracy and computation time are evaluated compared to conventional static and dynamic models. The results show that the proposed dynamic model estimates the same energy consumption as the traditional dynamic model for a computation time 85 times faster. The computation time of the static model is four times faster than the proposed model, but the accuracy is reduced.

**Keywords**—*Electric Vehicle, Electric Drive, Modeling, Simulation, Energetic Macroscopic Representation*

## I. INTRODUCTION

The transport sector must rapidly reduce its greenhouse gas emissions to face climate change. One possible solution is the electrification of road vehicles, such as Electric Vehicles (EVs). According to the International Energy Agency, 230 million EVs must be on the road in 2030 to limit climate change to 1.7°C [1]. To reach this target, the massification of the production of this kind of car is required. To reduce the EV time-to-market, fast, accurate, and flexible simulations are needed. Thus, developing appropriate models is essential to speed up the conception phase.

Different models or simulation tools can be chosen according to the conception objectives [2], [3]. A comparison between several simulation tools is proposed in [4]. In [5] and [6], the authors compare static and dynamic models of an electric drive for electric vehicles. The dynamic models of a traction drive are the most precise. However, they suffer from a high computational burden. Static models are computationally faster but less accurate.

The present paper proposes a fast-computational dynamic model for EVs. The objective of the proposed simplified model is to find a compromise between the accuracy of the dynamic model and the low computation time of the static one. To achieve this aim, the modeling choices and simulation solvers are discussed. Lastly, a comparison between the static, the classical dynamic and the proposed models is realized to validate the compromise between computation and accuracy.

These models will be organized using the Energetic Macroscopic Representation (EMR) formalism [7]. EMR is an organizational tool that highlights the energetic properties of systems. Flexibility is one of the advantages of the EMR [8]. It is easy and readable to switch from a static to a dynamic model of an electric drive, as shown in this paper. All simulations are carried out on the Matlab/Simulink software.

Section II develops the electric vehicle's modeling with the drive's static model. Section III focuses on the difference between the modeling of the two dynamic models. The simulations of the different drives are compared in Section IV. Section V sums up the difference between the models.

## II. ELECTRIC VEHICLE MODELING

### A. Studied Vehicle

The considered vehicle is the Peugeot e-208, a small segment electric car called B-segment in Europe (Figure 1) [9]. The vehicle has a mass of 1.6 Tons with the passengers. The car is composed of a 50 kWh Li-ion battery, and an electric drive which is an inverter connected to a 100 kW Permanent Magnet Synchronous Machine (PMSM). The electric drive is connected to the mechanical transmission and the wheels and mechanical brakes.



Figure 1: Peugeot 208 electric[9]

### B. Energetic Macroscopic Representation of the Vehicle with a static model for the electric drive

The different equations used in the complete model of the vehicle are presented from the sources to the road. The battery voltage  $u_{bat}$  depends on the battery resistance  $R_{bat}$ , the current of

the electric drive  $i_{ed}$ , and the Open Circuit Voltage  $u_{ocv}$ , which depends on the battery State of Charge (SoC).

$$u_{bat} = u_{ocv}(SoC) - R_{bat}i_{ed}. \quad (1)$$

A static model of the electric drive is used in this section. An efficiency map represents the variation of the losses in the drive  $\eta_{ed}$  as a function of the speed and the torque. The mechanical torque produced by the drive  $T_{ed}$  is imposed to be equal to the reference torque  $T_{ed\_ref}$  calculated by the control part. The current  $i_{ed}$  is defined by the power balance as expressed in Eq. (2), with  $\Omega_{mt}$ , the speed of the mechanical transmission.

$$\begin{cases} T_{ed} = T_{ed\_ref} \\ i_{ed} = \frac{T_{ed}\Omega_{mt}}{u_{bat}\eta_{ed}^k} \end{cases} \text{ with } k = \begin{cases} 1 & \text{if } T_{ed}\Omega_{mt} \geq 0 \\ -1 & \text{if } T_{ed}\Omega_{mt} < 0 \end{cases} \quad (2)$$

The mechanical transmission is modeled by Eq. (3) with  $T_{mt}$  its torque,  $k_{mt}$  the transmission ratio, and  $\eta_{mt}$ , its efficiency. The mechanical transmission speed  $\Omega_{mt}$  depends on the wheel speed  $\Omega_w$  and the transmission ratio.

$$\begin{cases} T_{mt} = T_{ed}k_{mt}\eta_{mt}^k \\ \Omega_{mt} = k_{mt}\Omega_w \end{cases} \text{ with } k = \begin{cases} 1 & \text{if } T_{ed}\Omega_{mt} \geq 0 \\ -1 & \text{if } T_{ed}\Omega_{mt} < 0 \end{cases} \quad (3)$$

The wheels are represented as an equivalent wheel because curves and wheels slips are assumed negligible. The wheel force  $F_w$  is equal to the mechanical transmission torque  $T_{mt}$  divided by the wheel radius  $R_w$ . The wheel speed depends on the vehicle speed  $v_{ev}$ .

$$\begin{cases} F_w = \frac{T_{mt}}{R_w} \\ \Omega_w = \frac{v_{ev}}{R_w} \end{cases} \quad (4)$$

The total force applied by the vehicle  $F_{tot}$  is the sum of the wheel force  $F_w$  and the mechanical brake force  $F_{br}$

$$F_{tot} = F_w + F_{br} \quad (5)$$

The vehicle speed is calculated using the Newton's Law with  $M_{ev}$  the total mass of the vehicle,  $F_{tot}$  the force applied by the vehicle and  $F_{res}$  the resistance force to vehicle forward motion.

$$v_{ev} = \frac{1}{M_{ev}} \int (F_{tot} - F_{res}) dt \quad (6)$$

The resistance force depends on the rolling resistance  $F_{roll}$  and the aerodynamic resistance  $F_{aero}$ .

$$F_{res} = F_{roll} + F_{aero} \quad (7)$$

The EMR of the EV is presented in Figure 2. The battery, the road, and the brakes are the different energetic sources represented by green ovals. The electric drive is a multi-physical energy conversion element represented by an orange circle. The mechanical transmission and the equivalent wheel are represented by an orange square (mono-physical energy conversion). Equations (5) and (6), which describe the chassis, are respectively represented by a coupling element (double

orange square) and an accumulation element (crossed orange rectangle).

The local control part can be deduced directly from the EMR (light blue elements). The accumulation is inverted indirectly. A controller  $C(s)$  in the Laplace transform formalism is considered to control the velocity, with "s" the Laplace variable. The closed-loop response time is 0.1 s which gives a good capture of the accelerations of the vehicle.

$$F_{tot\_ref} = F_{res\_mes} + C(s)(v_{ev\_ref} - v_{ev\_mes}) \quad (8)$$

Then, a distribution element splits the total force reference between the wheels and the brake through a distribution criterion  $k_{br}$  (9), given by the strategy (dark blue block). More details on the strategy can be found in [10].

$$\begin{cases} F_{br\_ref} = k_{br} F_{tot\_ref} \\ F_w\_ref = (1 - k_{br}) F_{tot\_ref} \end{cases} \text{ with } k_{br} \in [0, 1] \quad (9)$$

Finally, the wheels (10) and the mechanical transmission (11) are directly inverted to give the electric drive reference torque.

$$T_{mt\_ref} = R_w F_w\_ref \quad (10)$$

$$T_{ed\_ref} = \frac{T_{mt\_ref}}{k_{mt}} \quad (11)$$

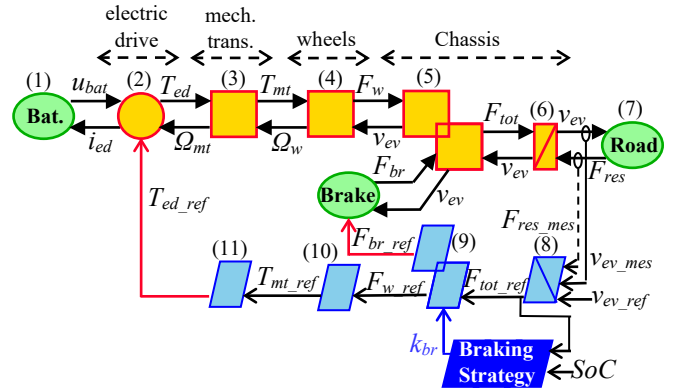


Figure 2: Energetic Macroscopic Representation of the EV with a static model for the electric drive (Bat.: Battery, mech. trans.: mechanical transmission)

The simulation of the static model is implemented in Matlab/Simulink, where a fixed-step solver is selected. A sampling frequency must be chosen for discrete systems to fulfill the system's stability in the Jury criterion, which is more restrictive than the Shannon theorem [11]. As the vehicle simulation is realized in discrete time, a step time of 20 ms (5 times faster than the control loop response time) is chosen to fulfill the Jury Criterion.

### III. DYNAMIC MODELS OF THE ELECTRIC DRIVE

In this Section, we consider the static model of the electric drive to be replaced by a dynamic one. It is composed of the model of the inverter, the model of the PMSM in the d-q

reference frame, and the control of the whole. The conventional model is presented first and simplified in the second part.

### A. Conventional Dynamic Model

The three arms inverter is firstly modeled. The voltages  $\underline{V}_{abc}=[V_a, V_b, V_c]^t$  are the products of the modulation vector  $\underline{m}_{abc}=[m_a, m_b, m_c]^t$  with the battery voltage  $U_{bat}$ . The current  $i_{ed}$  is linked with the modulation vector and the three-phase currents vector  $\underline{i}_{abc}=[i_a, i_b, i_c]^t$ . The inverter losses are calculated from the conduction and switching losses of the semiconductors [12], [13].

$$\begin{cases} \underline{V}_{abc} = \underline{m}_{abc} U_{bat} \\ i_{ed} = \underline{m}_{abc}^t \underline{i}_{abc} \eta_{inv}^k \end{cases} \quad (12)$$

The stator currents  $\underline{i}_{abc}$  and voltages  $\underline{V}_{abc}$  are expressed in the d-q frame  $\underline{i}_{dq}$  and  $\underline{V}_{dq}$  using the Park transformation matrix  $P(\theta)$  given by equation (14), where  $\theta$  is the position of the rotor flux.

$$\begin{cases} \underline{V}_{dq} = [P(\theta)] \underline{V}_{abc} \\ \underline{i}_{abc} = [P(\theta)]^{-1} \underline{i}_{dq} \end{cases} \quad (13)$$

$$P(\theta) = \sqrt{\frac{2}{3}} \begin{bmatrix} \cos(\theta) & \cos(\theta - \frac{2\pi}{3}) & \cos(\theta + \frac{2\pi}{3}) \\ -\sin(\theta) & -\sin(\theta - \frac{2\pi}{3}) & -\sin(\theta + \frac{2\pi}{3}) \end{bmatrix} \quad (14)$$

The currents  $i_d$  and  $i_q$  in the stator windings are a function of the voltages  $V_d$  and  $V_q$ , the inductors  $L_d$  and  $L_q$ , the stator resistance  $R_s$ , and the electromotive forces  $e_d$  and  $e_q$ .

$$\begin{cases} i_d = \frac{1}{L_d} \int (V_d - R_s i_d - e_d) dt \\ i_q = \frac{1}{L_q} \int (V_q - R_s i_q - e_q) dt \end{cases} \quad (15)$$

The electromotive forces  $e_d$  and  $e_q$  are linked to the inductors  $L_d$  and  $L_q$ , the currents  $i_d$  and  $i_q$ , the mechanical transmission speed  $\Omega_{mt}$ , the number of pole pairs  $p$ , and the rotor flux  $\Psi_r$  imposed by the permanent magnets.

$$\begin{cases} e_d = -p L_q i_q \Omega_{mt} \\ e_q = p \Omega_{mt} (L_d i_d + \Psi_r) \end{cases} \quad (16)$$

The machine torque  $T_{ed}$  is expressed as a function of the pole pair number, the inductors, the currents, and the rotor flux. The machine losses are added to the drive torque.

$$T_{ed} = p \left( (L_d - L_q) i_d + \Psi_r \right) i_q \eta_{EM}^k \quad (17)$$

The position of the rotor is given by the equation (18).

$$\theta = p \int \Omega_{mt} dt \quad (18)$$

The electric drive of the static model is replaced by the dynamic model (Figure 3). The inverter and the Park transformation are presented by a coupling element (orange square). The stator windings are represented by an accumulation element (crossed orange rectangle). Equations (12)-(14) are the electro-mechanic conversion of the drive (orange circle). The other blocks in the EMR are the same as the static model.

The control path of the dynamic electric drive (light blue blocks) is then realized, beginning with the inversion of the electro-mechanic conversion. As only one equation describes the currents  $i_d$  and  $i_q$  as a function of the torque, the current  $i_d$  is provided by a strategy.

$$\begin{cases} i_{d.ref} = i_{d.strat} \\ i_{q.ref} = \frac{T_{ed.ref}}{p \left( (L_d - L_q) i_{d.strat} + \Psi_r \right)} \end{cases} \quad (19)$$

The windings equations are inverted indirectly using two controllers  $C_d(s)$  and  $C_q(s)$ .

$$\begin{cases} V_{d.ref} = e_{d.mes} + C_d(s)(i_{d.ref} - i_{d.mes}) \\ V_{q.ref} = e_{q.mes} + C_q(s)(i_{q.ref} - i_{q.mes}) \end{cases} \quad (20)$$

The inversion of the Park transformation is then realized to obtain the three-phase voltages  $\underline{V}_{abc.ref}$ .

$$\underline{V}_{abc.ref} = [P(\theta)]^{-1} \underline{V}_{dq.ref} \quad (21)$$

Finally, the modulation ratios are calculated as the function of the three-phase voltages and the battery voltage.

$$\underline{m}_{abc} = \frac{\underline{V}_{abc.ref}}{U_{bat}} \quad (22)$$

The strategy gives the current  $i_d$  as a function of the Torque  $T_{ed}$  and the speed of the machine using a look-up table.

The EMR of the conventional dynamic model is implemented in Matlab/Simulink. To fulfill the Jury criterion, the control loop of the machine imposes a simulation step time of less than 0.2 ms. Thus, the traditional model used a fixed-step solver with a step time of 0.1 ms corresponding to the inverter frequency. As the control of the inverter is considered as using an average signal, it is sufficient for the simulation.

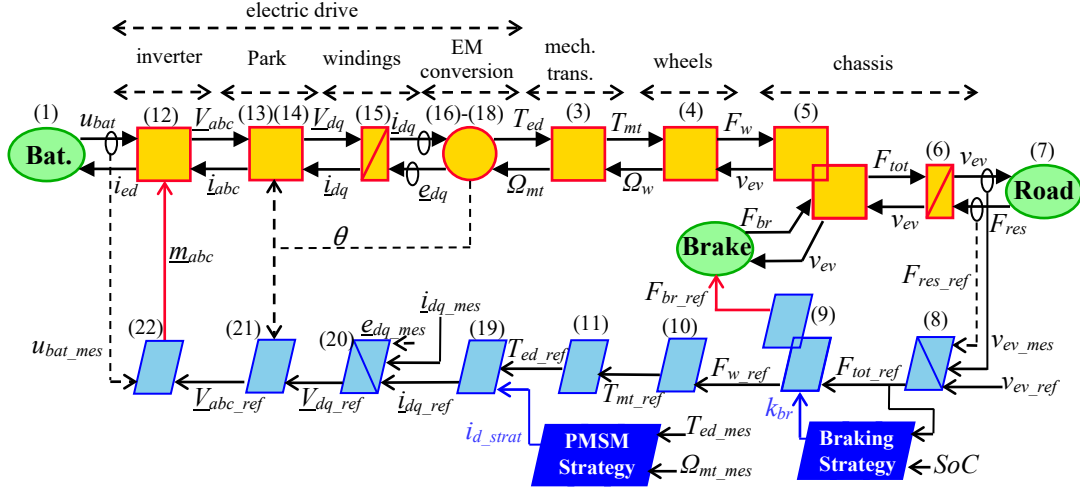


Figure 3: EMR of the conventional dynamic model of an EV (Bat.: Battery, EM conversion: electro-mechanical conversion, mech. trans.: mechanical transmission)

### B. Proposed Model Simplifications

In this model, the inverter and the Park transformation have been merged in one block. So, the equations (12)-(14) have become the following equation:

$$\begin{cases} V_{dq} = \underline{m}_{dq} U_{bat} \\ i_{ed} = \underline{m}_{dq}^t \dot{i}_{dq} \eta_{inv}^k \end{cases} \quad (23)$$

With  $\underline{m}_{dq} = [m_d, m_q]^t$ , the modulation ratios of the inverter in the d-q frame. The EMR of the electric drive for the simplified model is given in Figure 4. The inversion of the inverter is given by equation (24). This equation replaces equations (21) and (22) in the proposed model.

$$\underline{m}_{dq} = \frac{V_{dq\_ref}}{U_{bat}} \quad (24)$$

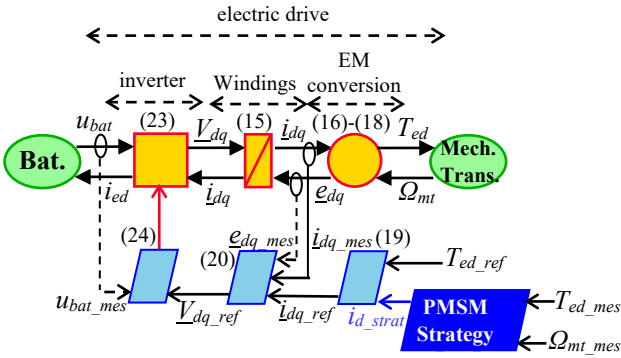


Figure 4: EMR of the proposed simplified model of the electric drive

The proposed model uses the variable step solver based on the modified Rosenbrock formula with a minimum step time of 20 ms. This solver is chosen because it can resolve stiff differential equations. Other stiff solvers on Matlab/Simulink or other software can give similar performances. This step time is the same as the static model, ensuring that the velocity profile and the vehicle acceleration are well computed in the simulation software. Thus, the variable solver allows allocating

only the computational effort when the variable states change. Consequently, the computation time is drastically reduced from minutes to seconds. This is not possible for the conventional model, as shown in Section IV.A.

### IV. COMPARISON OF THE DIFFERENT DRIVE MODELS

The simulations are carried out using the European homologation cycle, the WLTC class3 (Figure 5). The simulations are realized with a processor I7- 11<sup>th</sup> generation- 2.5 GHz on Matlab/Simulink 2021b.

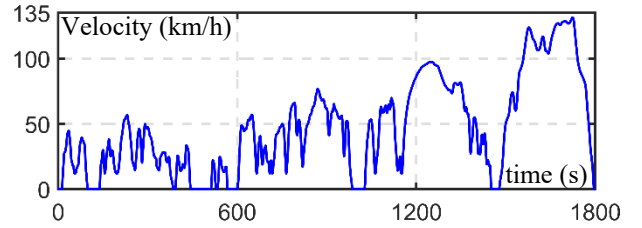


Figure 5: WLTC driving cycle

#### A. Comparison between the complete and simplified dynamic models

To explain the difference between the two models, the current  $i_q$  and one phase current  $i_a$  are respectively given in Figure 6 and Figure 7. The phase currents have been reconstructed from the calculated d-q currents. As conclusions are like the ones for  $i_a$ , other phase currents ( $i_b$  and  $i_c$ ) are not plotted here for lack of space.

The currents  $i_q$  are the same for the two models (Figure 6). The values of these currents are defined by the torque setpoint imposed by the velocity control loop (i.e., defined by the acceleration of the vehicle). For the simplified dynamic model, the variable solver only calculates more points when the rate of change of the currents between two sample times is too high.

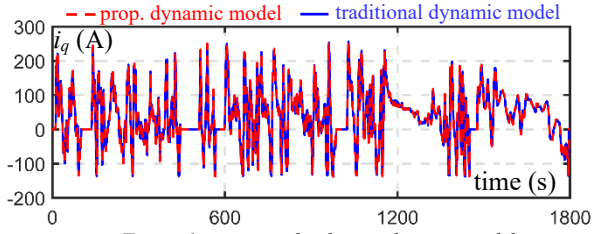


Figure 6: current  $i_q$  for the two dynamic models

For comparison over a broad time scale, it seems that the currents  $i_a$  calculated by the two models are the same (Figure 7). However, it is not the case when a zoom is realized. The conventional model shows a sinusoidal current waveform at around 200 Hz. To have enough points to obtain this signal, it is necessary to have a high sampling frequency. It is therefore not possible to increase the fixed-step time of the solver for the classical dynamic model. Conversely, the d-q model has only 4 points represented by circles as d-q currents vary much slower. For this model, the small-scale accuracy is lost, and only the envelope of the signals is kept. Note that reconstruction of real waveforms has no sense for this d-q model. Moreover, it is unnecessary as energetic calculations can be realized directly from d-q values with very good accuracy.

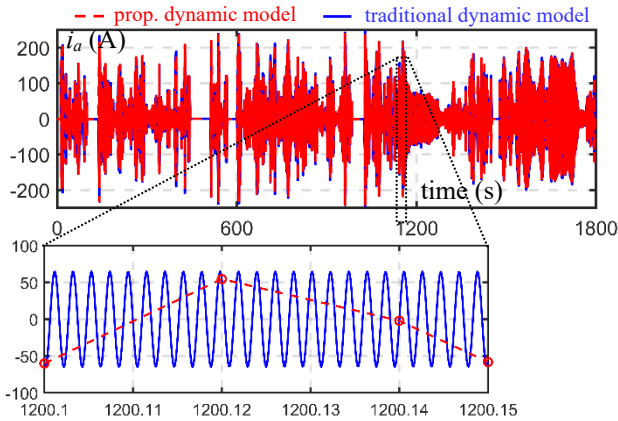


Figure 7: phase current  $i_a$  for the two dynamic models

### B. Comparison between the different models

The different models are compared regarding the accuracy of energy consumption estimation and computation time (Table 1). The power given by the battery and the energy consumption are presented in Figure 8 and Figure 9, respectively. The battery power for the two dynamic models is the same. For the static model, the power is a little bit higher. The energy consumption of the static model is 6 % higher than the two dynamic models, which have the same energy consumption. The proposed dynamic model reduced the computation time by 85 compared to the conventional one. The static model is the fastest one, with a computation time of less than 3s. However, the energy consumption prediction error is significant. The simplified dynamic model proposed is therefore an excellent approach combining the precision of the prediction and reduction of the computation time.

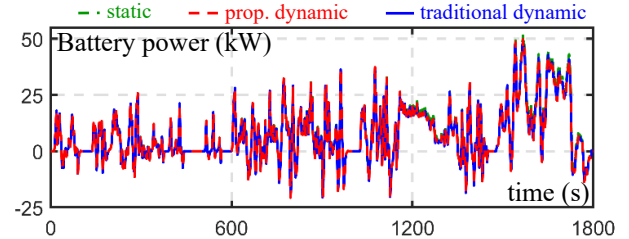


Figure 8: Comparison of the battery power for the three considered models

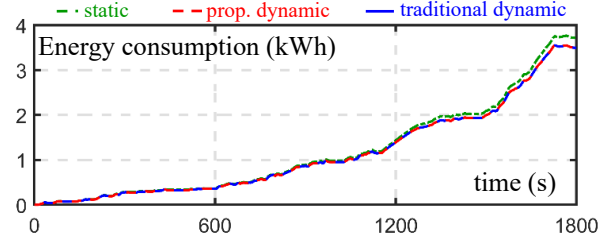


Figure 9: Comparison of the energy consumption for the different models

Table 1: Energy consumption and computation of the different models

	Static model	Proposed dynamic model	Conventional dynamic model
Energy consumption	3.717 kWh	3.497 kWh	3.497 kWh
Computation time	2.42 s	7.95 s	11 min 20s

## V. CONCLUSION

This paper proposes a simplified dynamic model for the electric drives of EVs. This model has the same accuracy as the conventional dynamic model and a considerable reduction in the needed computation time, which is reduced to a few seconds. This model is interesting to be used in the first step of developing EVs.

The next step of this work is to validate the proposed dynamic model with a real test on the electric machine. An evaluation of the vehicle's consumption for different driving profiles will also be realized.

## ACKNOWLEDGMENT

This work is performed under the collaborative STELLANTIS framework OpenLab "PSA@Paris-Saclay - Electrical engineering for Mobility."

## REFERENCES

- [1] "Global EV outlook 2021, Accelerating ambitions despite the pandemic" International Energy Agency report, 2021.
- [2] D. W. Gao, C. Mi, and A. Emadi, "Modeling and simulation of electric and hybrid vehicles," *Proceeding of the. IEEE*, vol. 95, no. 4, pp. 729–745, April 2007
- [3] D. D. Tran, M. Vafaeipour, M. El Baghdadi, R. Barrero, J. Van Mierlo, O. Hegazy, "Thorough state-of-the-art analysis of electric and hybrid vehicle powertrains: Topologies and integrated energy management strategies," *Renew. and Sustain. Energy Rev.*, vol. 119, n° 109596, 2020

- [4] C. Wayne Ng and L. Yossapong, "Comparison of Electric Bus Power Consumption Modelling and Simulation Using Basic Power Model, ADVISOR and FASTSim," *IEEE-SPIES'2*, 2020,
- [5] T. Letrouvé, A. Bouscayrol, W. Lhomme, N. Dollinger and F. Mercier Calvairac, "Different models of a traction drive for an electric vehicle simulation", *IEEE-VPPC'10*, September 2010.
- [6] A. Desrevelaux, M. Ruba, A. Bouscayrol, G. M. Sirbu and C. Martis, "Comparisons of models of electric drives for electric vehicles." *IEEE-VPPC'19*, October 2019.
- [7] A. Bouscayrol, J.-P. Hautier and B. Lemaire-Semail, "Graphic formalisms for the control of multi-physical energetic systems: Cog and emr," *Systemic design methodologies for electrical energy systems: analysis synthesis and management*, pp. 89-124, 2012.
- [8] D. Ramsey, A. Bouscayrol, L. Boulon, A. Desrevelaux, A. Vaudrey, "Flexible Simulation of an Electric Vehicle to Estimate the Impact of Thermal Comfort on the Energy Consumption," *IEEE Trans. On Transp. Elec.*, 2022, doi: 10.1109/TTE.2022.3144526.
- [9] Peugeot e-208 [online] Available: <https://www.peugeot.fr/nos-vehicules/e-208.html> Accessed: April 2022
- [10] A. Desrevelaux, A. Bouscayrol, R. Trigui, E. Castex and J. Klein, "Impact of the Velocity Profile on Energy Consumption of Electric Vehicles," *IEEE Trans. on Veh. Tech.*, vol. 68, no. 12, pp. 11420-11426, 2019.
- [11] M. S. Mahmoud, M. G. Singh, *Discrete systems: analysis, control and optimization*, Springer Science & Business Media, 2012.
- [12] B. Rolle et O. Sawodny, « Analytical Voltage-Source Inverter Current and Conduction Loss Models for EV Power Train Simulations,» *IFAC-PapersOnLine*, vol. 51, n° 31, p. 479-484, 2018,
- [13] Automotive inverter from Infineon [online] Available: <https://www.infineon.com/cms/en/product/power/igbt/automotive-qualified-igbts/automotive-igbt-modules/fs380r12a6t4b/> Accessed: April 2022